Study the influence of formulation process parameters on solubility and dissolution enhancement of efavirenz solid solutions prepared by hot-melt extrusion: a QbD methodology

Article (Accepted Version)

Study the influence of formulation process parameters on solubility and dissolution enhancement of Efavirenz solid solutions prepared by Hot melt Extrusion: a QbD methodology

Jaywant Pawar*[1], Dilipkumar Suryawanshi[1], Kailas Moravkar[1], Rahul Aware[2], Vasant Shetty[2], Mohammed Maniruzzaman[3], Purnima Amin[1]

1. Department of Pharmaceutical Sciences and Technology, Institute of Chemical Technology, UGC-CAS; Elite Status, N. P. Marg, Matunga, Mumbai 400019, India.
2. ACG Pharma Technologies Pvt. Ltd., Shirwal, Pune, Maharashtra, India.
3. Department of Pharmacy/Chemistry, School of Life Sciences, University of Sussex, Falmer, Brighton, BN1 9QJ

Corresponding author:

Pawar Jaywant Nivrutti

Senior Research Fellow

Department of Pharmaceutical Sciences and Technology,

Institute of Chemical Technology,

N. P. Marg, Matunga, Mumbai 400019, India.

Tel. +912233612211 Fax. +91 33611020.

E-mail address: jaywantpawar.ict@gmail.com

Graphical abstract

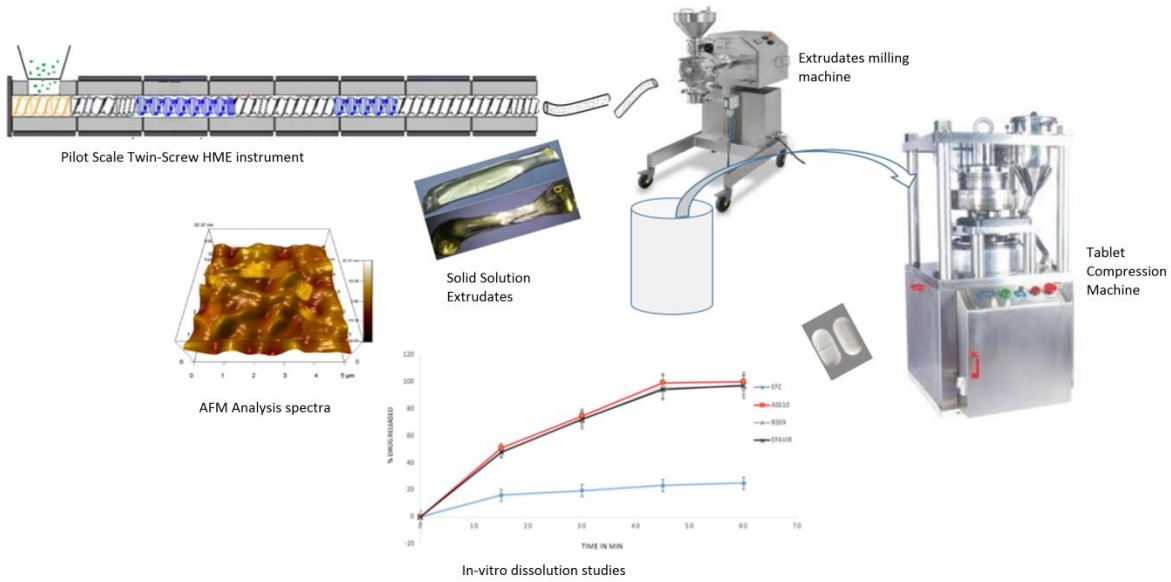

Abstract:

The current study investigates the dissolution rate performance of amorphous solid solutions of poorly water soluble drug, efavirenz (EFV) in amorphous Soluplus® (SOL) and Kollidon® VA64 (KVA64) polymeric systems. For the purpose of the study various formulations with varying drug loadings of 30% 50% and 70 % w/w were developed via hot-melt extrusion processing and adopting a Box-Behnken design of experiment (DoE) approach. The polymers were selected based on the Hansen solubility parameters calculation and the prediction of the possible drug-polymer miscibility. In DoE experiments, Box Behnken factorial design was conducted to evaluate effect of independent variables such as , Soluplus® ratio (A_1), HME screw speed (A_2), and processing temperature (A_3); Kollidon®VA64 ratio (B_1), screw speed (B_2),and processing temperature (B_3) on responses such as solubility (X_1 and Y_1), dissolution rate (X_2 and Y_2) for both ASS [EFV:SOL] and BSS [EFV:KVA64] systems. DSC and XRD data confirmed that bulk crystalline EFV transformed to amorphous form during the HME processing. Advanced chemical analyses conducted via 2D COSY NMR, FTIR chemical imaging, AFM analysis and FTIR showed that EFV was homogenously dispersed in the respective polymer matrices. The maximum solubility and dissolution rate was observed in formulations containing 30% EFV with both SOL and KVA64 alone. This could be attributed to the maximum drug-polymer miscibility in the optimized formulations. The actual and predicted values of both responses were found precise and close to each other.

Key words

Box Behnken design, Hot-melt extrusion, Efavirenz**,** solubility enhancement**,** 2D COSY NMR

Abbreviations:

Efavirenz: EFV

Solid solution: SS

Hot-melt extrusion : HME

Soluplus :SOL

Kollidon® VA64 : KVA64

Box-Behnken Design : BBD

Sodium lauryl sulfate: SL

1. Introduction

Efavirenz (EFV) is used as a first line therapeutic drug for HIV-I and is a specific non-nucleoside reverse transcriptase inhibitor. EFV is a white crystalline powder, belongs to class II of biopharmaceutical classification system (BCS) and exhibit very poor solubility and dissolution rate which results into very low and variable oral bioavailability [1-3]. Whilst, EFV is the most promising chemical entity against HIV-I therapy, the limited solubility and thus bio-availability makes the successful delivery of this drug very challenging. Therefore, there is an immense need for the implementation of a suitable formulation strategy to overcome the issues associated with poor water solubility of EFV.

Hot-melt extrusion (HME) has become a well-known processing technology in the development and manufacturing of amorphous solid dispersion or solid solution systems. In such systems a crystalline drug is covered into amorphous form or a molecularly dispersed system is formed [4]. In recent years combinatorial chemistry and high throughput screening has resulted into rise in the number of poorly water soluble drugs found in pharmaceutical discovery pipeline [5]. Sufficient aqueous solubility and bioavailability is needed for optimum oral absorption of a drug candidate. As a result, scientists from industry as well as academia are working together on several aspects of solubility enhancements of challenging drug candidates to tackle the growing and unmet need.

Amorphous solid solutions or solid dispersions are known as highly supersaturated category of drug delivery systems. These systems have attracted a lot of research interests, due to the ability of these systems to facilitate an improved solubility and oral bioavailability of poorly water-soluble crystalline drugs [6, 7]. The glassy molecular dispersion of drug in an amorphous polymer matrix is termed as solid solutions (SS). In order to form a miscible and thermodynamically stable molecular system, one has to consider complete miscibility of the drug in a suitable polymeric system below its saturation solubility, and therefore drug-polymer miscibility is of great importance for the development of the concept of SS [8, 9]. In the present context, instead of traditional methods for the preparation of SS such as solvent evaporation, and spray drying techniques, we have used HME as the most promising solvent-free, continuous and industry feasible and scalable process for the preparation of EFV SS [10]. We are reporting preparation of EFV solid solutions by HME technology using two widely used thermostable amorphous polymers; Soluplus® (SOL) (polyvinyl caprolactam polyvinyl acetate polyethylene glycol graft copolymer) and Kollidon® VA64 (KVA64) (Vinylpyrrolidone-vinyl acetate copolymer) by adopting a Quality by Design (QbD) approach. Both polymers are amphiphilic in nature that can work as solubilizing agent and have been reported in the literature for dissolution enhancement of other poorly water soluble drugs[11-13].

Response surface methodology (RSM), is one of the techniques used to study possible effects, their interactions on shape of response surface and quadratic effects for formulation optimization. The Box-Behnken Design (BBD) is a method to understand effect of formulation variables (independent factors) on their effect on formulation responses (dependent variables) as shown in fishbone diagram (Fig.1). BBD is considered to be more efficient and most powerful than other designs such as central composite design, three level full factorial design due to the fact that it requires fewer experimental runs compared to other techniques, hence it is less expensive [14]. The experimental treatment combinations are placed at midpoints of edges and at center of process space, giving higher percentage yields as well as less treatment time with minimum costs [15]. Drug-polymers miscibility has been investigated by the Hansen solubility parameter (HSP). The HSP calculation is a tool for the theoretical predication of drug-polymer miscibility at preformulation stage prior to the HME processing [16]. In this

study, we have demonstrated BBD as a part of RSM technique to study the effects of processing parameters for the formulation of solid solutions (SS) of Efavirenz (EFV) using HME.

2. Material and methods:

2.1 Materials

Efavirenz (EFV) was a kind gift from Laurus Labs, India. Both Soluplus and Kollidon VA64 were kindly donated by BASF Corporation, Mumbai, India. Marketed sample of EFV tablets AVIRANZ® (100 mg) was purchased from retailers shop in Mumbai, India. All other chemicals and solvents used were of analytical grade and were procured from SD fine Chemicals, Mumbai, India. Milli-Q water was used throughout the study.

2.2 Box Behnken Factorial design:

Box-Behnken design with 3 factors, 3 levels was employed to develop EFV SS systems. The HME experimental design and data analysis was conducted using licensed version of Design expert® software (version 9.0.4.1; M/s, Stat-Ease, Minneapolis, USA). The adopted Box-Behnken design resulted in 13 runs each for both polymers and wereused for optimization study (Fig.1 is in supplementary information). Three factors such as different polymer ratios, variable screw speed and variable temperature of the process were used as independent variables for preparation of SS. A full quadratic model was fitted to collect responses, and P values and were used to determine their effect on HME process [19]. The effect of independent variables [SOL ratio (A_1), variable screw speed (A_2) and variable temperature (A_3)] as well as [KVA64 ratio (B_1), variable screw speed (B_2) and variable temperature (B_3)] on dependent variable [Solubility (X_1 & Y_1) and dissolution rate enhancement (X_2 & Y_2)], where (X refers to SOL and Y refers to KVA64) in EFV SS were studied as shown in Table 1.
The linear equation of the model is as follows:

$$Y = b_0 + b_1A_1 + b_2A_2 + b_3A_3 + b_{12}A_1A_2 + \ldots\ldots..b_nX_n \quad \text{Eq. [I]}$$

Where Y is the response, $b0$ is the constant and b_1 b_2 …… b_n is the coefficient of factor A_1, A_2… A_n …as well as …... B_1, B_2… B_n. is representing the effect of each ordered within -1, +1.

The DoE software designed 13 experimental runs for each polymer respectively as mentioned in Table 2. One-way ANOVA and multilinear regression analysis were performed to test the significance of Box- Behnken model and factor coefficients. As per ICH guideline, Q8 outlines different terms and steps involved in EFV SS tablet manufacturing process, all steps involved in this study are shown in (Fig.1 in supplementary information).

2.3 HME process to manufacture solid solutions (SS) of EFV

EFV SS formulations were prepared using single-screw Lab Hot Melt Extruder (S.B. Panchal and Co., India) equipped with stainless steel single screw with diameter of 24.5mm and length of 5.8 inch. The barrels have feeder, conveyer, mixing sections, and carrier zone with internal diameter 25.5mm and length of 6 inch attached with a round shaped die (2 mm in diameter). The processing temperatures were selected based on Tg of polymers and melting point of EFV in order to obtain transparent extrudates which were further termed as solid solutions (SS). The obtained extrudes of EFV SS were stored in a desiccator at room temperature for further physicochemical characterization. The drug loading was kept constant 30% as shown in and independent variables i.e. polymer ratios were varied as shown in Table 2. All 26 batches were processed as recommended by DoE runs. The different weight ratios of polymer to drug, different temperature processing ranges from 110°C - 140°C were applied to

obtain semi-solid, transparent extrudates for each formulation suitable for downstream processing of EFV SS to formulate tablet dosage form.

The optimized batches ASS10 and BSS9 specified by DoE were further processed on a production scale pilot Twin-screw HME instrument (ACG Pharma Machinery Pvt. Ltd. India) with batch size of 500gm each. The obtained extrudates were further milled using Multimill (ACG Pharma Tech, India). The milled granules stored in airtight containers until further physicochemical characterization.

2.3.1 Downstream processing of EFV SS granules to form tablets:

The prepared granules each from optimized batch i.e. **ASS10** and **BSS9** of EFV SS of 500gm each were further compressed using a Rimek Tablet compression machine to form tablets with dose equivalent to 100mg of EFV.

2.4 Physicochemical characterization of EFV ASDs

2.4.1 Saturation solubility study

Saturation solubility study was carried out for neat EFV and SS of EFV in 2% sodium lauryl sulfate (SLS) distilled water maintained at 37 ± 0.5 °C by adding excess quantities of API and SS were added to 10 ml of dissolution media and capped glass test tubes were kept in a shaking hot tub (Boekel scientific, USA) at 37±0.5°C, 30 rpm for 72 hrs. The supernatant solution was then filtered through 0.45µm millipore membrane filter and suitably diluted and analyzed for drug content in triplicate using UV-visible spectroscopy.

2.4.2 In vitro dissolution studies

The dissolution studies were conducted using a USP type II dissolution apparatus. The EFV SS tablets equivalent to 100 mg of API were placed in dissolution medium within apparatus for 60 min along with pure EFV and marketed tablet formulation (100mg dose). The dissolution medium was 2% sodium lauryl sulfate (SLS) in distilled water; 900 mL maintained at 37 ± 0.5 °C (pH of about 4.5 to 5.5) and the paddle rotation speed was 50 rpm. SS tablets equivalent to 100 mg of EFV were taken along with pure EFV drug (100 mg) subjected to same dissolution study [3]. At various time points like 5, 15, 30, 45 and 60min, the 10 ml of respective samples were withdrawn and an equal amount of fresh preheated medium 37 ± 0.5 °C was added to ongoing dissolution medium vessel. These samples were analysed using UV-spectrophotometer at 248 nm. The dissolution studies were performed in triplicate.

2.4.3 Differential Scanning Calorimetry (DSC)

DSC analysis was performed to check the solid state of the drug in the manufactured SSwith respect to pure EFV, SOL and KVA64 and optimized batches of ASS10 and BSS9 using Pyris-6 DSC Perkin Elmer (USA). The samples equivalent to 3-4 mg of was hermetically sealed in aluminum pan. The samples were then heated from 30°C - 300°C at rate of 10°C/min^{-1} under an inert atmosphere using purging nitrogen gas at a flow rate of 17-18 ml/min. An empty aluminum pan was used as a blank. The Pyris® manager software was used for post experimental analysis.

2.4.4 X-ray powder diffraction (PXRD) analysis

PXRD was used to determine the solid state of EFV SS made from extrudates along with other bulk materials using a Bruker D8 Advance in theta–theta mode. For PXRD study of SS, a Cu anode at 40 kV and 20 mA current was set, Soller slits (0.04 rad) were used in incident and diffracted beam path at sample rotation set at 15 rpm. Each sample was scanned from 2 to

50° 2 θ with a step size of 0.02° 2θ and a counting time of 0.3 seconds per step. The samples were placed in a zero background sample holder and incorporated on a spinner stage.

2.4.5 Structural analysis by FTIR

FTIR analysis was undertaken to investigate the molecular structures of EFV, SOL, KVA64, ASS10, and BSS9. The samples were analyzed for their functional group identification using Shimadzu MIRACLE IR Affinity-1 FTIR spectrophotometer. The samples were premixed with KBr using mortar and pestle and KBr disks were prepared by means of a hydraulic press. The scanning range was 4000 to 400 cm^{-1} with resolution of 4 cm^{-1}.

2.4.6 FTIR Spectroscopic Imaging

Fourier transform infrared imaging was conducted on a continuous scan spectrometer coupled with a macro sample chamber (Hyperion 3000, Bruker Optics GmbH, Ettligen, Germany) and a Focal Plane Array (FPA) detector 128 × 128, (Santa Barbara Focal plane, Goleta, California) at range: 4000-900 cm^{-1}. The thin film of extrudate obtained by cutting a rod of extrudates using a sharp razor of ASS10 was placed on crystal accessory; position of accessory was adjusted so that a good focused image could be obtained. The images were acquired with a spectral resolution of FTIR 8cm^{-1}, and 32 co-added scans with the help of OPUS® 6.5 software with an acquisition time of approximately 2min.

2.4.7 Atomic force microscopy (AFM) characterization

Sample for AFM was prepared by cutting the freshly prepared extrudates with smooth surfaces (Cross section of extrudates) by a razor blade. All extrudates with cylindrical rods of 20 mm and 50 mm were selected, and placed on a glass slide. The sample was placed such that it should keep its position horizontally, as this is required to get non-destructive imaging by atomic force microscope operations [20, 21]. AFM analysis was carried out using AFM instrument of DFRT-PFM on a commercial SPM system (Asylum Research MFP-3D, California, USA) with a nitrogen flow cell positioned above an inverted optical microscope. AFM with accelerating voltage up to ± 220 V and imaging at AC voltages up to 110 Vpp (in the dual-excitation mode) at frequencies of 300–400 kHz. Voltages were applied between the ITO substrate and the conductive probe tips, and AFM's preamplifier (Asylum Research ORCA head model59) recorded current. The light source used in the AFM instrument is superluminescent diode (SLD), classified as Class 1M light source [22]. This enables polarization switching in extrudes samples and imaging of samples with maximum resolution and magnification. An AFM scans the surface of a specimen with a sharp tip mounted to a cantilever (Olympus TR400PB cantilevers), the deflections are directly related to surface micro scale topography and its physical properties [20, 23]. Height, phase and amplitude images were collected simultaneously; using Platinum-coated, contact-mode AFM tips were used. The result data was processed using Open user interface based on IGOR Pro software with OpenGL® 3D for advanced image display.

2.4.8 1H COSY or 2D NMR analysis

The 2D COSY NMR experiments were carried out on prepared SS i.e. ASS10 and BSS9 using a Varian Mercury Plus 300 NMR spectrometer operated at 300

MHz with cross polarization contact time of 1 ms, pulse repeat time of 1 s, accumulation of 1000 scans, and high-power 1H-decoupling of 100 kHz during signal acquisition with a - 80º to 130 º with suitable solvent. Sufficient SS powder sample was dissolved in solvent DMSO and then used for analysis [23, 24]. Sample was spun at a rate of 5 kHz at magic angle with 2D width 4807.7 Hz. 5 mm multi nuclear CP-MAS probe for solids application was used. Data processing was carried out using sine bell software with FT size 2048 × 2048 and for total time of 65 min.

2.4.9 Analytical method (HPLC)

The assay of the ASDs was assessed using high-performance liquid chromatography (HPLC) system of JASCO corporation equipped with auto sampler (AS-2055 plus, intelligent sampler), photodiode array detector (JASCO corp.). A Phenomenex Luna® reverse-phase C18 column (150 x 4.6 mm; 5µm particles) was used as a stationary phase. The mobile phase was composed of a mixture of buffer (Ammonium acetate buffer, pH maintained at 7.5): acetonitrile in the ratio 40:60 (v/v). The buffer was prepared by dissolving ammonium acetate in 1000 mL of water; maintain the pH at 7.5 ± 0.05. The flow rate was 1.5 mL/min, with injection, volume was 20 µL and the detection of EFV was done at 248 nm with the retention time of 3.38 ± 0.05min. Drug content uniformity was assessed by accurately weighing ASDs equivalent to 10 mg of EFV were dissolved in 10 mL of methanol and appropriately diluted. These samples further centrifuged (Centrifuge Eppendorf) for 5 min at 5000 rpm and drug content was quantified using previously delineated HPLC procedure.

3. Result and discussions

3.1 Design of Experiments (DoE)

3.1.1 Polymer selection for EFV SS formulation

The miscibility of any drug with a polymer can be outlined via utlizing molecular orientation based Hoftyzer and Van Krevelen method by means of solubility parameters calculation [17]. The solubility parameter difference Δδ between API and polymer provides possible idea on the miscibility of a particular drug and polymer system [18]. If solubility parameter difference is less than 7 $MPa^{1/2}$, itis generally accepted as an indication of miscibility whereas for a difference of more than 10 $MPa^{1/2}$ the system is likely to be immiscible. The underlying concept of the foregoing claim is based on the prediction that the energy of mixing required for the intermolecular interaction between a drug and polymer will be balanced by the intramolecular interactions with in the corresponding drug or polymer. EFV is a poorly soluble drug, having melting point 139 – 140°C with high crystallinity. As reported in literature EFV shows solubility parameters (δ) value of 24.55 in $MPa^{1/2}$. Whereas SOL and KVA64 shows solubility parameters (δ) value of 19.60 $MPa^{1/2}$ and 19.43 $MPa^{1/2}$ [13],respectively. This indicates that the the difference in the solubility parameters (δ) value in EFV/SOL and EFV/KVA64 systems as 4.95 and 5.12, respectively, which outlines the possibility of the formation of miscible systems, hence were proceeded further with the HME processing.

3.1.2 Box-Behnken Experimental Design

A three factor, three levels BBD was used to study the effect of different ratios of SOL as well as KVA64, temperature profiles and screw speed on dissolution rate and solubility enhancement of EFV SS. The experimental results i.e. response data for all experiments are given in Table 2. The ratio of maximum to minimum amount of each polymer i.e. SOL and

KVA64 were varied from 30 % to 70% for each. The values of responses for SOL (X_1= Solubility in mg/mL), (X_2= Dissolution rate in percentage) varies from lowest to highest values ranging from 0.987 ± 0.41 to 1.79 ± 0.97 mg/mL and 63.35 ± 4.09 to 100.2 ± 1.97 % whereas for KVA64 (Y_1= Solubility in mg/mL), (Y_2= Dissolution rate in percentage) varies from lowest to highest values ranging from 0.984 ± 0.59 to 1.702 ± 0.72 mg/mL and 48.32 ± 2.39 to 96.32 ± 3.67 %.

The ratio of maximum to minimum for both of two responses is 1.83 to 1.42 and 1.92 to 1.53, respectively, concluding there is no requirement of any power transformation. Usually a value of 10 is a difference that indicates requirement of power transformation. In general term, a moderately flat line indicates lack of dependence of response on the said factor [25].

3.1.3 Polynomial equations and response surface analysis

Two-dimensional contour plots and 3D surface plots were prepared for all three responses of each independent factor viz. variable ratios of SOL and KVA64, variable screw speed and different temperature and are depicted in Fig. 2. The independent factor and response variables were correlated using a polynomial equation with statistical analysis via Design-Expert® software which confirms that the most significant factors affecting responses are ratio of SOL and KVA64, variable screw speed and variable temperatures.

Analysis of variance (ANOVA) was applied to determine effects of variables and their interactions on responses. Final mathematical model in terms of coded factors as determined by Design-Expert® software are as follows.

$$\boldsymbol{X_1} = +81.69 + 13.10*A1 + 0.72*B+1.80*C - 41.37*ABC+0.65*A+0.028*B+0.051*\text{Eq. (III)}$$

$$\boldsymbol{X_2} = +1.42 + 0.27*A1-0.046*B - 2.75*C + 0.87*ABC + 0.013*A - 1.85*B - 7.85*C\text{Eq. (IV)}$$

$$\boldsymbol{Y_1} = +71.92+18.24*A2 +2.08*B+1.84*C+14.58*ABC+0.91*A+0.083*B+0.052*C \quad \text{Eq. (V)}$$

$$\boldsymbol{Y_2} = +1.36 +0.34*A2 + 9.16*B+0.017*C +0.41ABC+0.017*A +3.66*B + 4.74*C \quad \text{Eq. (VI)}$$

Where, $\boldsymbol{X_1}$ is solubility and $\boldsymbol{X_2}$ is dissolution rate of SS made from SOL, $\boldsymbol{Y_1}$ is solubility and $\boldsymbol{Y_2}$ is dissolution rate of SS made from KVA64. A1 is ratio of SOL, B1 is ratio of KVA64, B is variable screw speed and C is different temperature respectively as independent factors.

The polynomial equations include interaction term and related higher order effects and coefficients for intercept. A positive sign of coefficient indicate a synergistic effect while negative term indicates an antagonistic effect upon the respective response. The result from ANOVA tables for variable responses subsequently confirms fitness of model (i.e. $F < 0.05$) (please see the supplementary information). The mathematical relationships, generated using multiple linear regression analysis, has been used to generate counter plots for independent factors [26]. The resultant counter plots for all factors and responses are shown in Fig 2. A relatively flat line in the plots shows lack of dependence of response on the respective independent factors [25].

3.1.4 Effect of independent factors on saturation solubility (X_1 and Y_1) study

The responses (X_1 and Y_1) i.e. solubility values of EFV SS, is highlighted as either a decrease or an increase in solubility of EFV SS. When the coefficients of factor A (i.e. higher concentration of SOL) is positive, the highest processing temperature and optimum screw speed showed maximum solubility of SS. The results of solubility study of EFV SS prepared by HME showed increase in drug solubility with higher SOL and KVA64 ratio. The solubility of neat EFV in dissolution medium i.e. 2% SLS solution was found about 0.198 ± 0.81 mg/mL and in case of SS, the solubility values were found much higher in SS which was increasing with the increase in the concentration of both SOL and KVA64 processed at maximum barrel

temperature. The increase in apparent solubility of drug was may be attributed due to formation of complete amorphous solid solution of EFV [27]. The hydrophilic polymers processed via HME leads to increase in wettability of drug by decreasing surface tension of SS. As can be seen inFig. 4, the response surface 3D plot and contour plots shows effect of independent variables on responses of EFV SS solubility values. The 3D surface plots inferred that when SOL as well as KVA64 ratio was used in least ratio and at minimum screw speed, it then leads to lower solubility values.

3.1.5 Effect of independent factors on Dissolution rate (X_2 and *Y_2) studies*

In case of response *(X_2* and *Y_2),* positive coefficients of factor B (i.e. higher concentration of SOL and KVA64) showed maximum dissolution rate of EFV SS. In contrast, a negative coefficient of factor A (i.e. higher concentration of both polymers) showed better dissolution rate. The dissolution profile curves of bulk EFV, optimized batches of EFV ASS10, BSS9 and Marketed product of EFV are depicted in Fig.3. EFV is a poorly water soluble drug with a solubility of only 5.2 ± 2.3 µg/mL in water (1). All the dissolution rate values and dissolution graph in percentages have been shown in supplementary data file of page number 1 and 2. The glassy solid solution of EFV ASS10 and BSS9 showed highest solubility and dissolution rate because of drug particles being molecularly dispersed in respective polymer matrices resulting into formation of SS amorphous system [28]. The dissolution rate and solubility might be increased due to its increased wettability, greater hydrophilicity, improved dispersibility and reduction in particle size of the bulk drug. The ASS10 and BSS9 exhibited similar drug release profiles to that of the marketed tablets with values at about 100, 96 and 97%, respectively. As per the DoE runs, different processing conditions showed different solubility as well as dissolution rate values attributed to the effect of independent variables on the responses.. The differences in dissolution rate among all ASDs seen may be due to solubilisation nature of polymers, their different ratios, screw speed, barrel temperature as mentioned in the DoE study (Table 3) which is in resemblance with previously published literature for other poorly water soluble drugs processed by hot melt extrusion [29, 30].

3.1.6 DoE post analysis and optimization of EFV SS

The DoE optimization study was carried out to find out level of independent factors A1 (ratio of SOL and A2 (ratio of KVA64) B (screw speed) and C (Barrel temperature) which had predicted results such as $\boldsymbol{X_1}$ as 1.725 ± 0.1890 mg/mL and $\boldsymbol{X_2}$ as 96.53 ± 1.247% similarly $\boldsymbol{Y_1}$ as 1.725 ± 0.075 mg/mL and $\boldsymbol{Y_2}$ as 94.02 ± 2.278 %. (As shown in Fig.4) The experimental values of the results were found as similar as predicted values. The results inferred that the batch processed at 70% of SOL and KVA64 at 140° C temperature and 75 screw speed had given the best results. To validate the experimental models, the optimized formulation was prepared in triplicate by using these values of independent factors and the results are shown in average of three with standard deviation values.

The Fig. 4 shows the optimized EFV SS overlay plots by DoE software, stating the effect of different independent factors on solubility and dissolution rate improvement of EFV SS prepared using SOL and KVA64 as carriers.

3.2 DSC analysis

DSC analysis of EFV, SOL, KVA64, ASS10 and BSS9 formulations was carried out to study the melting temperature and recrystallization behaviour of the crystalline drug. Fig. 3 in supplementary material showed DSC thermograms of all components, which also evaluates the drug-polymer miscibility and amorphicity of the manufactured extrudates. EFV was characterized by the Enthalpy (ΔH) and a single, sharp melting endothermic peak 102.16 J/g

and 139.60°C, respectively, whereas SOL and KVA64 did not show any melting endotherm because of their amorphous nature. SS formulations of EFV showed a complete decrease in ΔH and exhibited no melting endotherms indicating an amorphous existence of the drug. The DSC findings are in accordance with the PXRD results [31]. Moreover, the drug polymer miscibility was determined by analyzing the DSC samples at various polymer ratios. The physical mixtures of EFV and polymers showed an endotherm peak between 137 – 142°C which is attributed to the presence of the crystalline drug in the blends whereas the SS formulations showed no thermal peak of EFV indicating complete conversion of EFV into amorphous form. This result illustrates that crystalline nature of EFV was reduced using HME technology, by converting it into a stable SS using a polymers like SOL and KVA64.

3.3 XRD analysis

The cryallinity outputs via XRPD analysis of the formulations are summarized in Fig. 4 in supplementary material which shows the diffractograms of pure EFV, SOL, KVA64, ASS10 and BSS9 formulations. EFV exhibited characteristic sharp peaks at diffraction angle (2θ) values of 6.11°,10.43°, 10.98°, 12.27°, 13.25°, 14.20°, 16.92°, 20.14°, 21.25°, and 24.93°, data resembles with literature [32] which indicates the highly crystalline state of the bulk drug. Both SOL and KVA64 showed no intensity peaks and thus confirms their amorphous nature. The melt extrudate SS formulations showed absence of characteristics peak at respective 2θ angles of pure EFV, which became too broaden and a heap like peaks, which infers a reduction of the crystallinity of the drug. From XRD results of SS formulations it has been proved that EFV has been converted to its amorphous form during the high shear HME processing when combined with amorphous polymeric carriers.. The findings are in good agreement with the DSC results. The SS formulations which are technically an amorphous system that contain additional free energy resulting in the solubility enhancement of EFV compared to its bulk form [33].

3.4 FTIR analysis

The Fourier transform infrared spectroscopy is usually used to study the intermolecular interactions between components for the formation of stable amorphous solid solution [34, 35]. The FTIR spectra of EFV, SOL, KVA64, ASS10 and BSS9 are summarized in Fig. 5 in supplementary material. The FTIR spectra of EFV showed characteristics band at 3314 cm^{-1} (for NH stretch vibration), 1742 cm^{-1} (C=O stretching vibration), 1492 cm^{-1} (C≡C of benzene ring stretching vibration), 1240 cm^{-1} (CN stretch), 1165 cm^{-1} (CO stretching vibration), 1096, 1057, 1074cm^{-1} (C-O-C stretch vibration) and 689 and 652 cm^{-1} (-CF stretch) [36]. In case of both polymers SOL, KVA64 showed characteristics broad band around 3000-3500 cm^{-1}, C=O stretch at 1738 cm^{-1} and 1632 cm^{-1}, and aliphatic C-H stretch at 2932 cm^{-1} recognized for presence of maximum number of –OH stretching groups. The hydrogen bond formation between drugs and polymers has been shown by weak interactions observed at 1033 cm^{-1} [27, 37]. The carbonyl peaks assigned to free and hydrogen-bonded carboxylic acid C=O appeared at 1681 cm^{-1} and 1730 cm^{-1} in infrared spectra of crystalline EFV, but in case of SS formulations these peaks were found shifted from original ketone stretch of 1730 cm^{-1}. This infers that the strength of intermolecular interaction may have exhausted in case of crystal lattice. Additional hydrogen bond formation was found with hydroxyl group of each polymers with EFV resulting into a broad peak at 3158 cm^{-1} [38]. Both polymers showed maximum number of hydrophilic groups giving maximum hydrophilic surface resulting into diffusion of dissolution medium and accelerated release of EFV SS. Both EFV SS formulations showed very similar IR spectra indicated by shifting and broadening of peak of EFV compared to that of bulk EFV. Ambrogi (2012) et. al. has reported that, formation of hydrogen bond due to weak

interactions between drug and polymers can be easily wrecked in biological fluids and result into fast drug release higher solubility for the developed formulations [39].

3.5 AFM analysis

The AFM analysis of EFV SS with respect to their homogeneity was carried out using AFM analysis. The results are illustrated in Fig. 5a-d. The molecular level roughness data are depicted in Fig 5 a & c while 3D surface image in Fig. 5 b & d. The AFM images were determined for illustrating the extrudates morphological surface interactions in detail. The phase images illustrated that there is no phase separation between both components indicating EFV has been adsorbed uniformly by both polymers SOL and KVA64 [22]. Cross sectional and 3D Topography views of AFM analysis of ASS10 and BSS9 showed that there is high level of surface interaction between both components each leading to amorphosization of drug inside polymer system [22, 23]. Molecular solid solution at homogeneous state is directly related with amorphousness of SS systems. Both extrudates showed complete transparent solid solution as well as molecular homogeneity. The findings confirm that the AFM images showed different molecular structure roughness in the cross-sectional extrudates (Fig 5 b & d).

3.6 FTIR chemical imaging analysis

FTIR imaging results have been summarized in Fig. 6. The 3D image and IR reflectance spectrum of the point of interest of HME SS with 30% w/w loading of EFV specifies the surface compositional homogeneity. Use of FTIR imaging spectrum provides detailed information of SS at the molecular level which has been reported in literature (40, 41). FTIR imaging was constructed basically both on light reflectance and compositional difference at surface of samples. The homogeneity of EFV in SOL system as illustrated in chemical images, considerably marked intensity of FTIR reflectance spectrum in region of 1630 to 1740 cm^{-1} for amorphous EFV. The band at 1725 cm^{-1} corresponds to carbonyl group of EFV; H-bonded to hydroxyl group of SOL [40, 42]. The 3D graph is illustrated by homogeneity of EFV by orange - red color and SOL by yellow-green color. From the results of FTIR chemical imaging analysis, the homogeneity of EFV in SOL matrices was confirmed. The findings are also complemented by the DSC and XRD analyses.

3.7 2D COSY NMR analysis:

The 2D COSY NMR analysis of EFV ASS10, BSS9 has been shown in Fig. 7a and (Fig.7b in the supplementary file). From the results it can inferred that, cross peaks between molecular protons within a coupling network were detected at protons range of δ 1.0 – 14.0 of ASS10 and δ 1.0 – 12.0 in BSS9. The stability of solid-state EFV in the amorphous solid solution is attributed to the drug-polymer interactions and its amorphous molecular mobility is well illustrated by the 2D COSY NMR studies [23]. In case of ASS10, there is proton-proton coupling observed at various point such as δ 0.8 to 1.0, 1.1 to 1.6, 3.4 to 3.6, 6.1 to 6.6 and 7.45 to 7.6 which states the molecular interaction between the EFV and SOL[43]. The resonance peaks specific of EFV and both polymers were detected with coupling shifts due to the proton resonances. Similarly for BSS9 of EFV with KVA64,characteristic cross peaks in the coupling network at δ 0.5-1.1, 0.5-1.7, 1.1-1.7, 7.1-7.6, 1.15-6.6 and 7.6-7.7 were observed. This proton-proton coupling indicates a high level of molecular interaction between EFV and KVA64. Moreover, all characteristics drug peak frequencies were observed in SS formulation that confirms the stable structural and physico-chemical state of EFV in all formulations [13].

3.8 Drug content by HPLC analysis

The HPLC drug content analysis of EFV via HPLC and method validation was carried out as per ICH and FDA guidelines. The linear calibration curve of EFV was plotted with concentrations in range of 10-200 µg/mL, with coefficient of regression (R^2) value of 0.997. In HPLC analysis, retention time for EFV was found ~3.38 ± 0.05min. The percent relative standard deviation (RSD) of the replicate was found less than 2%, demonstrating relative reproducibility of this method. After extrusion, each SS systems were analyzed for drug content using HPLC. The results of drug content have been shown in supplementary material. The SS samples equivalent to 20 µg/mL were taken from each batch for drug content analysis. All SS fell within the acceptable range i.e. 95% to 105% of drug content as per US Pharmacopoeia for EFV tablets. It was found that the drug content of the optimized ASS10 and BSS9 were found about 98.02 and 100.34%, respectively. The standard deviation value of the formulations was in range between 0.99 and 2.23 % for all the EFV SS batches. This illustrated that HME processing conditions revealed excellent content uniformity of EFV in all the formulation batches.

Conclusions

In this context, EFV solid solutions were prepared using SOL and KVA64 as an amorphous polymeric carriers using Box Behnken design model. An HME technique was utilized for the optimization of EFV SS formulation and process variables. The solid-state analyses of EFVconducted by means of DSC. PXRD, FTIR, AFM and FTIR imaging confirmed the formation of amorphous dispersions of the drug in both polymer matrices . The crystalline EFV was converted to amorphous state during the extrusion process due to the high shear force generated during the processing of the formulations. The dissolution rate of EFV in the developed EFV SS formulations were significantly higher than that of the marketed product. About 100% drug was released in less than one hour, whereas marketed formulation took 60 minutes to show 100% drug release. SOL showed the highest solubility and dissolution rate at higher processing temperature and optimum screw speed. Hydrogen bonding between polymer and EFV played an important role in the increase in the solubilization of EFV and thus the dissolution enhancement which was then confirmed by both the FTIR and 2D COSY NMR analyses. In conclusion, it can be claimed that a QbD approach was adopted to develop and optimize amorphous solid dispersion of poorly water soluble drug EFV in order to enhance its dissolution rate and the solubility.

Acknowledgments

The authors would like to acknowledge Laurus Labs, Hyderabad, India, for genuine gift sample of Efavirenz. The author is thankful to Dr. Rahul Aware and Vasant Shetty from ACG Machines Pvt. Ltd. For allowing there twin-screw HME facility at Pune, India. Authors is thankful to university grants commission India for providing the research fellowship. The authors are thankful to S.A.I.F., Department at Indian Institute of Technology, Mumbai for FTIR imaging analysis and 2D COSY analysis of the samples.

Conflict of Interest: The authors report no conflicts of interest

References

1. Maurin, M. B., Rowe, S. M., Blom, K., & Pierce, M. E. (2002). Kinetics and mechanism of hydrolysis of efavirenz. Pharm Res. 19(4), 517-521.
2. Takano, R., Sugano, K., Higashida, A., Hayashi, Y., Machida, M., Aso, Y., & Yamashita, S. (2006). Oral absorption of poorly water-soluble drugs: computer simulation of fraction absorbed in humans from a miniscale dissolution test. Pharm Res, 23(6), 1144-1156.
3. Sathigari, S. K., Radhakrishnan, V. K., Davis, V. A., Parsons, D. L., & Babu, R. J. (2012). Amorphous-state characterization of efavirenz—polymer hot-melt extrusion systems for dissolution enhancement. J Pharm Sci, 101(9), 3456-3464.
4. Crowley, M. M., Zhang, F., Repka, M. A., Thumma, S., Upadhye, S. B., Kumar Battu, et.al. (2007). Pharmaceutical applications of hot-melt extrusion: part I. Drug Dev Ind Pharm, 33(9), 909-926.
5. Maniruzzaman, M., Nair, A., Renault, M., Nandi, U., Scoutaris, N., Farnish, R. et. al. (2015). Continuous twin-screw granulation for enhancing the dissolution of poorly water soluble drug. Int J Pharm, 496(1), 52-62.
6. Sun, D. D., & Lee, P. I. (2015). Probing the mechanisms of drug release from amorphous solid dispersions in medium-soluble and medium-insoluble carriers. J Contr Rel, 211, 85-93.
7. Yu, L. (2001). Amorphous pharmaceutical solids: preparation, characterization and stabilization. Adv Drug Deliv Rev, 48(1), 27-42..
8. Knopp, M. M., Tajber, L., Tian, Y., Olesen, N. E., Jones, D. S., Kozyra, A. et.al. (2015). Comparative study of different methods for the prediction of drug–polymer solubility. Mol Pharms, 12(9), 3408-3419.
9. Tian, Y., Booth, J., Meehan, E., Jones, D. S., Li, S., & Andrews, G. P. (2012). Construction of drug–polymer thermodynamic phase diagrams using Flory–Huggins interaction theory: identifying the relevance of temperature and drug weight fraction to phase separation within solid dispersions. Mol Pharm, 10(1), 236-248.
10. Shah, S., Maddineni, S., Lu, J., & Repka, M. A. (2013). Melt extrusion with poorly soluble drugs. Int J Pharm, 453(1), 233-252.
11. Djuris, J., Ioannis, N., Ibric, S., Djuric, Z., & Kachrimanis, K. (2014). Effect of composition in the development of carbamazepine hot-melt extruded solid dispersions by application of mixture experimental design. J Pharm Pharmacol, 66(2), 232-243.
12. Li, M., Gogos, C. G., & Ioannidis, N. (2015). Improving the API dissolution rate during pharmaceutical hot-melt extrusion I: Effect of the API particle size, and the co-rotating, twin-screw extruder screw configuration on the API dissolution rate. Int J Pharm, 478(1), 103-112.
13. Fule, R., Paithankar, V., & Amin, P. (2016). Hot melt extrusion based solid solution approach: Exploring polymer comparison, physicochemical characterization and in-vivo evaluation. Int J Pharm, 499(1), 280-294.
14. Marasini, N., Yan, Y. D., Poudel, B. K., Choi, H. G., Yong, C. S., & Kim, J. O. (2012). Development and optimization of self-nanoemulsifying drug delivery system with enhanced bioavailability by Box–Behnken design and desirability function. J Pharm Sci, 101(12), 4584-4596.
15. Abdelbary, A. A., & AbouGhaly, M. H. (2015). Design and optimization of topical methotrexate loaded niosomes for enhanced management of psoriasis: application of Box–Behnken design, in-vitro evaluation and in-vivo skin deposition study. Int J Pharm, 485(1), 235-243.
16. Maniruzzaman, M., Morgan, D. J., Mendham, A. P., Pang, J., Snowden, M. J., & Douroumis, D. (2013). Drug–polymer intermolecular interactions in hot-melt extruded solid dispersions. Int J Pharm, 443(1), 199-208.
17. Van Krevelen, D. W., & Te Nijenhuis, K. (2009). Properties of polymers: their correlation with chemical structure; their numerical estimation and prediction from additive group contributions. Elsevier.

584 18. Greenhalgh, D. J., Williams, A. C., Timmins, P., & York, P. (1999). Solubility parameters
585 as predictors of miscibility in solid dispersions. J Pharm Sci, 88(11), 1182-1190.
586 19. Maddineni, S., Battu, S. K., Morott, J., Soumyajit, M., & Repka, M. A. (2014). Formulation
587 optimization of hot-melt extruded abuse deterrent pellet dosage form utilizing design of
588 experiments. J Pharm Pharmacol, 66(2), 309-322.
589 20. Lauer, M. E., Siam, M., Tardio, J., Page, S., Kindt, J. H., & Grassmann, O. (2013). Rapid
590 assessment of homogeneity and stability of amorphous solid dispersions by atomic force
591 microscopy—from bench to batch. Pharmaceutical research, 30(8), 2010-2022.
592 21. Tho, I., Liepold, B., Rosenberg, J., Maegerlein, M., Brandl, M., & Fricker, G. (2010).
593 Formation of nano/micro-dispersions with improved dissolution properties upon dispersion of
594 ritonavir melt extrudate in aqueous media. Eur J Pharm Sci, 40(1), 25-32.
595 22. Lauer, M. E., Grassmann, O., Siam, M., Tardio, J., Jacob, L., Page, S., Alsenz, J. (2011).
596 Atomic force microscopy-based screening of drug-excipient miscibility and stability of solid
597 dispersions. Pharm Res, 28(3), 572-584.
598 23. Fule, R., Dhamecha, D., Maniruzzaman, M., Khale, A., & Amin, P. (2015). Development
599 of hot melt co-formulated antimalarial solid dispersion system in fixed dose form
600 (ARLUMELT): Evaluating amorphous state and in vivo performance. Int J Pharm, 496(1),
601 137-156.
602 24. Zhou, P., Xie, X., Knight, D. P., Zong, X. H., Deng, F., & Yao, W. H. (2004). Effects of
603 pH and calcium ions on the conformational transitions in silk fibroin using 2D Raman
604 correlation spectroscopy and 13C solid-state NMR. Biochem, 43(35), 11302-11311.
605 25. Mahesh, K. V., Singh, S. K., & Gulati, M. (2014). A comparative study of top-down and
606 bottom-up approaches for the preparation of nanosuspensions of glipizide. Powd Technol, 256,
607 436-449.
608 26. Kaur, P., Singh, S. K., Garg, V., Gulati, M., & Vaidya, Y. (2015). Optimization of spray
609 drying process for formulation of solid dispersion containing polypeptide-k powder through
610 quality by design approach. Powd Technol, 284, 1-11.
611 27. Pawar, J. N., Shete, R. T., Gangurde, A. B., Moravkar, K. K., Javeer, S. D., et.al. (2016).
612 Development of amorphous dispersions of artemether with hydrophilic polymers via spray
613 drying: Physicochemical and in silico studies. Asi J Pharm Sci, 11(3), 385-395..
614 28. Hancock, B. C., & Parks, M. (2000). What is the true solubility advantage for amorphous
615 pharmaceuticals?. Pharm Res, 17(4), 397-404.
616 29. Alshahrani, S. M., Lu, W., Park, J. B., Morott, J. T., Alsulays, B. B., Majumdar, et. al.
617 (2015). Stability-enhanced hot-melt extruded amorphous solid dispersions via combinations of
618 Soluplus® and HPMCAS-HF. AAPS PharmSciTech, 16(4), 824-834..
619 30. Pawar, J., Tayade, A., Gangurde, A., Moravkar, K., & Amin, P. (2016). Solubility and
620 dissolution enhancement of efavirenz hot melt extruded amorphous solid dispersions using
621 combination of polymeric blends: A QbD approach. Eur J Pharm Sci, 88, 37-49.
622 31. Sarode, A. L., Sandhu, H., Shah, N., Malick, W., & Zia, H. (2013). Hot melt extrusion
623 (HME) for amorphous solid dispersions: predictive tools for processing and impact of drug–
624 polymer interactions on supersaturation. Eur J Pharm Sci, 48(3), 371-384.
625 32. Alves, L. D. S., Soares, M. F. D. L. R., de Albuquerque, C. T., da Silva,et. al. (2014). Solid
626 dispersion of efavirenz in PVP K-30 by conventional solvent and kneading methods. Carbohyd
627 Polym, *104*, 166-174.
628 33. Meer, T., Fule, R., Khanna, D., & Amin, P. (2013). Solubility modulation of bicalutamide
629 using porous silica. J Pharm Inv, 43(4), 279-285.
630 34. Sinclair, W., Leane, M., Clarke, G., Dennis, A., Tobyn, M., & Timmins, P. (2011). Physical
631 stability and recrystallization kinetics of amorphous ibipinabant drug product by Fourier
632 transform Raman spectroscopy. J Pharm Sci, 100(11), 4687-4699.

633 35. Ueda, H., Muranushi, N., Sakuma, S., Ida, Y., Endoh, T., Kadota, K., et. al. (2016). A
634 strategy for co-former selection to design stable co-amorphous formations based on
635 physicochemical properties of non-steroidal inflammatory drugs. Pharm Res, 33(4), 1018-
636 1029..
637 36. Gaur, P. K., Mishra, S., Bajpai, M., & Mishra, A. (2014). Enhanced oral bioavailability of
638 efavirenz by solid lipid nanoparticles: in vitro drug release and pharmacokinetics studies.
639 BioMed Res Int, 2014.
640 37. Rumondor, A. C., Stanford, L. A., & Taylor, L. S. (2009). Effects of polymer type and
641 storage relative humidity on the kinetics of felodipine crystallization from amorphous solid
642 dispersions. Pharm. Res., 26(12), 2599.
643 38. Ueda, K., Higashi, K., Yamamoto, K., & Moribe, K. (2013). Inhibitory effect of
644 hydroxypropyl methylcellulose acetate succinate on drug recrystallization from a
645 supersaturated solution assessed using nuclear magnetic resonance measurements. Mol.
646 Pharm., 10(10), 3801-3811.
647 39. Ambrogi, V., Perioli, L., Pagano, C., Marmottini, F., Ricci, M., Sagnella, A., et. al. (2012).
648 Use of SBA-15 for furosemide oral delivery enhancement. Eur. J. Pharm. Sci, 46(1), 43-48.
649 40. Feng, X., Vo, A., Patil, H., Tiwari, R. V., Alshetaili, A. S., Pimparade, M. B., et. al. (2015).
650 The effects of polymer carrier, hot melt extrusion process and downstream processing
651 parameters on the moisture sorption properties of amorphous solid dispersions. J Pharm
652 Pharmacol.
653 41. Alhijjaj, M., Bouman, J., Wellner, N., Belton, P., & Qi, S. (2015). Creating drug
654 solubilization compartments via phase separation in multicomponent buccal patches prepared
655 by direct hot melt extrusion–injection molding. Mol Pharm, 12(12), 4349-4362.
656 42. Kyerematen, S. O., Pudlas, M., & Woehrle, G. H. (2014). A fast and reliable empirical
657 approach for estimating solubility of crystalline drugs in polymers for hot melt extrusion
658 formulations. J Pharm Sci, 103(9), 2847-2858.
659 43. Pham, T. N., Watson, S. A., Edwards, A. J., Chavda, M., Clawson, J. S., Strohmeier, M.,
660 et.al. (2010). Analysis of amorphous solid dispersions using 2D solid-state NMR and 1H T 1
661 relaxation measurements. Mol Pharm, 7(5), 1667-1691.

662